

## Characterization of Ferritic Ductile Cast Irons Modified by W and Nb Additions

Gülşah Aktaş ÇELİK<sup>1\*</sup>, Şeyda POLAT<sup>1</sup>, Ş. Hakan ATAPEK<sup>1</sup>,  
G. N. HAİDEMENOPOULOS<sup>2,3</sup>

<sup>1</sup>Kocaeli University, Department of Metallurgical and Materials Engineering, Kocaeli, Turkey

<sup>2</sup>University of Thessaly, Department of Mechanical Engineering, Laboratory of Materials, Volos, Greece

<sup>3</sup>Khalifa University of Science and Technology, Department of Mechanical Engineering, UAE

### Keywords:

ThermoCalc  
SiMo ductile cast  
iron  
Alloy design,  
Characterization

### Abstract

The aim of this study was to develop ferritic ductile cast irons as alternative exhaust manifold materials to commercial SiMo alloy using elements like W and Nb in place of Mo. In the compositional design, Thermo-Calc software was used to follow all the phase transformations at equilibrium and obtained results were compared with the commercial SiMo alloy. Calculations revealed several alloy carbides such as M<sub>6</sub>C and MC depending on the presence of Mo, W and Nb within the composition. The calculated critical transformation temperatures shifted to higher ones by the usage of W and Nb in place of Mo and higher Si. The designed compositions were then cast and their microstructural features were characterized by several metallurgical analyses. The examinations on the cast alloys showed that; (i) microstructural features i.e. ferritic matrix, graphite, carbides were present within the solidified structure as predicted, (ii) graphite morphology varied according to the alloying element and Nb strongly deteriorated graphite morphology by changing it from spheroidal to irregular spheroidal and vermicular.

## W ve Nb İlavesi ile Modifiye Edilmiş Ferritik Sünek Dökme Demirlerin Karakterizasyonu

### Anahtar Kelimeler:

ThermoCalc  
SiMo dökme demir  
Alaşım tasarımı  
Karakterizasyon

### Özet

Bu çalışmanın amacı, ekzoz manifoldu olarak kullanılan ticari SiMo alaşımlarına alternatif ferritik sünek dökme demirlerin Mo yerine W ve Nb kullanımı ile geliştirilmesidir. Kimyasal kompozisyon tasarımında dengedeki bütün faz dönüşümlerinin izlenmesi için Thermo-Calc yazılımı kullanılmış ve elde edilen bulgular ticari SiMo alaşımı ile karşılaştırılmıştır. Hesaplamalar, kompozisyonda bulunan Mo, W ve Nb alaşım elementlerine bağlı olarak M<sub>6</sub>C ve MC gibi karbürlerin oluştuğunu göstermiştir. Hesaplanan kritik dönüşüm sıcaklıkları W ve Nb kullanımının yanı sıra, artırılmış Si içeriği ile daha yüksek değerlere kaymıştır. Tasarlanan kompozisyonlar döküm yoluyla üretilmiş ve mikroyapısal özellikleri çeşitli metalurjik analizlerle belirlenmiştir. Deneysel çalışmalar (i) hesaplamalar ile tahmin edildiği gibi mikroyapının ferritik matriks içerisinde grafit ve karbürlerden oluştuğunu, (ii) grafit morfolojisinin alaşım elementine bağlı olarak değiştiğini ve Nb katkısının grafit morfolojisini küreselden vermiküle doğru değiştirdiğini göstermiştir.

## 1. INTRODUCTION

Ductile cast irons are used for many applications in the automotive industry since they have relatively low cost and their mechanical, thermal and chemical properties can be improved according to the requirements [1, 2]. For exhaust manifold applications, a ferritic ductile cast iron having high conductivity, low thermal expansivity, sufficient mechanical properties and improved oxidation resistance was developed through modifications with alloying elements Si and Mo [2, 3]. Silicon addition provides solid solution strengthening of the ferrite matrix and makes it stable at elevated temperatures. In addition, Si provides oxidation resistance by forming Si-rich oxide layer [1-7]. Mo is usually added to ferritic ductile iron to improve the high-temperature mechanical properties by dispersion strengthening mechanism [1-7]. However, literature indicate that the usage of these elements is limited since ductility decreases substantially as Si content increases above 5 wt.-% and Mo addition above 1.0 wt.-% causes brittleness and shrinkage defects [2]. Therefore, SiMo ductile cast iron usually has silicon between 3.5 - 4 wt.-% and molybdenum between 0,6 - 0.8 wt.-% [8-10]. This usage limits the maximum service temperature of SiMo and therefore it cannot meet increasing demand in power density of engines [9-12]. In order to develop maximum service temperature of ferritic ductile cast irons, it is beneficial to add some alloying elements (i.e. Al, Nb, W, Ti etc.) which increase the transformation temperature from ferrite to austenite ( $A_1$ ) [13].

In this study, ferritic ductile cast irons containing W and Nb alloying elements were developed using CALPHAD (CALculation of PHase Diagrams) approach, to be used in place of commercial SiMo alloy at higher service temperatures. The developed alloys were cast and characterized together with a commercial SiMo alloy and the results were compared with thermodynamic calculations.

## 2. EXPERIMENTAL STUDY

In this study, initially thermodynamic calculations were carried out using the compositions given in Table 1 and in the second stage designed compositions were cast and their microstructural features were evaluated and compared with a commercial SiMo alloy.

**Table 1.** The compositions used in ThermoCalc calculations (wt.-%)

Specimen	C	Si	W	Nb	Mo
SiMo	3,4	3,6	-	-	0,8
SiW	3,5	4,00	1	-	-
SiNb	3,5	4,00	-	1	-

In thermodynamic calculations, ThermoCalc software with TCFE6 database was used. The C isopleths were obtained for all studied compositions thus, all phase transformations and their equilibrium temperature were determined from liquid phase to room temperature (RT). Phases stable at RT were also determined for all studied compositions.

The designed alloys were produced according to ASTM A 536 - 84 standard as Y block by sand mold casting. For casting, the charges consisting of nodular pig iron, ferrosilicon, ferrotungsten / ferroniobium and DIN 1020 were melted in the 35 KW Inductotherm induction furnace. Melting process was completed at 1560 °C and spheroidization process was carried out in a SiC crucible by using nucleation agent and magnesium rich alloy FeSiMg for spherodization. After spherodization, a sample from the molten alloy was taken by pouring it into a copper mold, in order to verify the chemical composition by Optical Emission Spectrometer (OES, Foundry Master). The rest of the molten metal was cast into a sand mold. Table 1 shows the chemical compositions of the cast alloys and the commercial SiMo alloy. The compositions are coded as specimen SiW and SiNb for 1 wt. % W and Nb additions, respectively.

**Table 2.** Chemical compositions of the cast alloys obtained by OES (wt. %)

Specimen	C	Si	W	Nb	Mo	Mg	Mn	P	S
SiMo	3,32	3,52	-	-	0,81	0,049	0,13	0,031	0,008
SiW	3,57	4,04	0,96	-	-	0,074	0,23	0,057	0,028
SiNb	3,46	3,96	-	0,97	-	0,082	0,23	0,059	0,028

For microscopic examinations, as cast alloys were prepared by metallographic methods. Microstructural characterization was carried out using both light microscope (LM, Olympus BX41M-LED) and scanning electron microscope (SEM, Jeol JSM 6060). Phases present were also identified by x-ray diffraction (XRD, Rigaku Ultima+). XRD studies were carried out with Cu-K $\alpha$  radiation and at a scanning speed of 1.0 °/min. The determined phases were quantified according to ISO 945-2 by image analyzer (IA, Leica Las V4.12).

### 3. RESULTS and DISCUSSION

#### 3.1. Thermodynamic Calculations

The C isopleths obtained by ThermoCalc software are given in Figure 1 for SiMo, SiW and SiNb alloys. According to the SiMo isopleth (Fig. 1a), graphite (G) crystallized directly from liquid (L) at 1250 °C and the crystallization temperature was also denoted as liquidus temperature ( $T_L$ ) for the studied composition. At 1180 °C, another crystallization, namely austenite (A), from liquid occurred. A eutectic reaction was observed at 1150 °C and the reaction produced austenite and M<sub>6</sub>C carbide. Several studies on this alloy composition indicated that the formed carbide was Mo-rich and one of the components of lamellar structure [3]. The initial formation of ferrite (F) from austenite occurred at 820 °C and this formation was completed at 800 °C which was designated as the A<sub>1</sub> temperature for SiMo alloy. This temperature is important since it determines the maximum temperature that the alloy can be used safely. According to this calculation, the final microstructure of SiMo alloy consisted of ferrite, M<sub>6</sub>C (Mo-rich carbide) and graphite. With the addition of W, the isopleth showed significant differences compared to SiMo alloy as given in Figure 1b. In SiW alloy, although the initial crystallization of graphite from liquid occurred similarly, the reaction took place at a higher  $T_L$  (1320 °C) due to the not only higher Si content but also W addition. Austenite solidification started from liquid at 1180 °C and was completed at 1150 °C. In contrast to SiMo alloy, W-rich M<sub>6</sub>C precipitated from austenite at 950 °C, rather than liquid phase in this alloy. Initial crystallization of ferrite was observed at 900 °C and ended at 852 °C which was designated as the A<sub>1</sub> temperature of SiW alloy. The reason for the higher A<sub>1</sub> temperature of SiW compared to SiMo alloy could be attributed to higher Si content and presence of W. Similar to SiMo alloy, designed microstructure of SiW consisted of ferrite, graphite and W-rich instead of Mo-rich M<sub>6</sub>C carbide. Figure 1c shows the C isopleth for SiNb alloy and the components like both graphite and austenite formed as a result of crystallization from liquid. The crystallization temperatures for graphite and austenite were obtained as 1320 °C and 1280 °C, respectively. Unlike to SiMo and SiW alloys, MC carbide crystallized directly from liquid at 1250 °C and by the completion of this crystallization, solidification was extended to 1200 °C. Crystallization of primary carbides from liquid takes place in ferro alloys having microalloying elements like Nb, Ti and V [13]. According to the isopleth, initial formation of ferrite from austenite started at 950 °C and was completed at 853 °C which is designated as the A<sub>1</sub> temperature for this alloy. Ferrite, graphite and Nb-rich MC carbide were present in the final microstructure at RT.

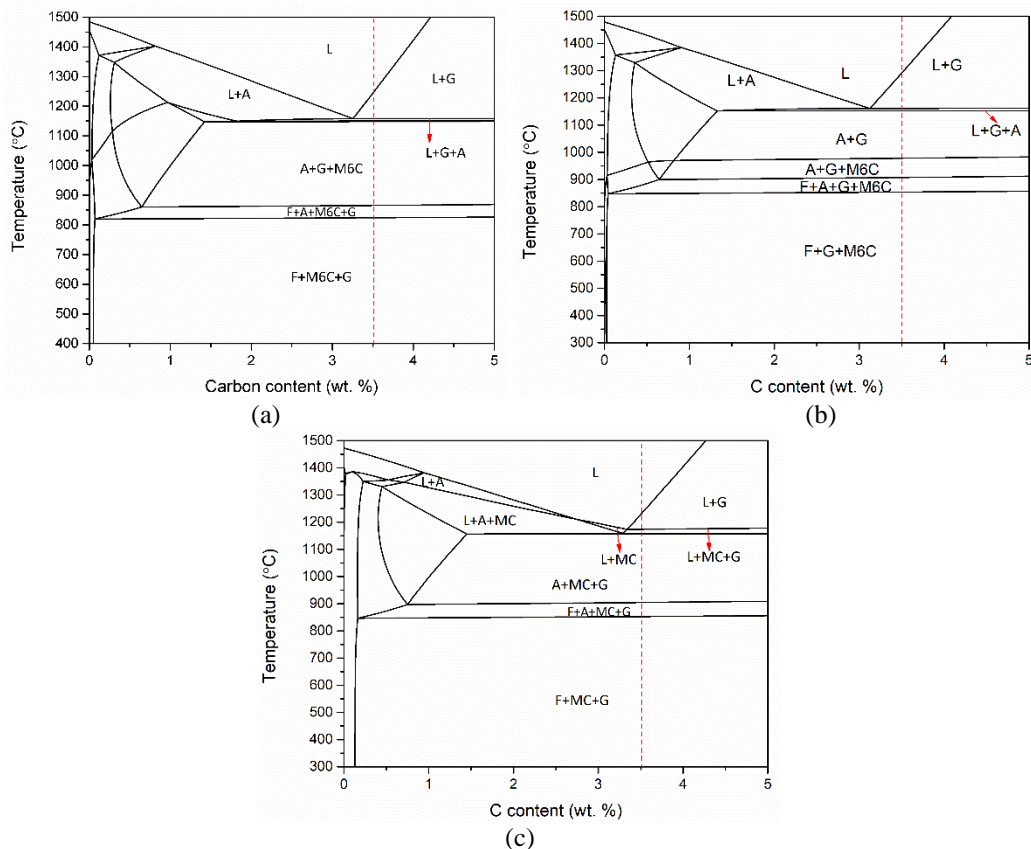


Figure 1. C isopleths of (a) SiMo, (b) SiW and (c) SiNb.

### 3.2. Metallurgical Analyses of Cast Alloys

General microstructures of the cast irons are given in Figure 2. All cast irons have three microstructural features as indicated by ThermoCalc results in Figure 1; (i) graphite, (ii) carbide/pearlite and (iii) matrix phase, ferrite. Image analysis was carried out in order to investigate the graphite morphology and quantitative data are given in Table 3. According to the results, SiMo has the highest amount of spheroidal graphite and the lowest amount of vermicular graphite. The data also show that, irregular spheroidal graphite increases in SiW with the addition of W. SiNb has the lowest amount of spheroidal graphite and the highest amount of vermicular graphite. Previous studies indicated the detrimental effect of Nb on the nodularity of the graphite [14, 15], as observed in this study. Figure 2 also shows the precipitation of carbides surrounded by pearlite in intercellular region. During solidification, Mo, W and Nb have low solubility in austenite therefore they partly segregate and solidify in intercellular regions, promoting carbide precipitation [4]. In order to identify the phases, SEM images showing the detailed microstructures of the alloys and EDS results taken from carbides are given Figure 3, 4 and 5. SEM image and EDS results given, show that SiMo has Mo-rich  $M_6C$  eutectic carbide surrounded by granular cementite (Fig. 3a and b) while SiW has W-rich  $M_6C$  carbide and granular precipitates (Fig. 4a and b) and SiNb has faceted Nb-rich MC carbide with cementite precipitates (Fig. 5a and b). XRD patterns of the alloys given in Figure 6 indicate that all cast irons have ferritic matrix as predicted by thermodynamic calculations (Fig. 1).

In addition to microstructural characterization, hardness values of cast irons were also determined and are given in Table 4. All cast irons have similar hardness values when standard deviations are considered, this is due to the equal amounts of carbide forming elements (Mo, W, Nb) and also similar content of Si which is responsible for solid solution hardening.

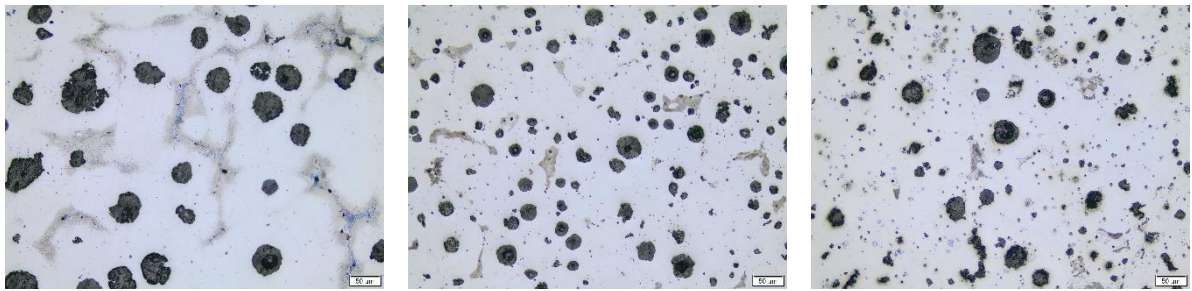
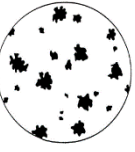
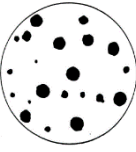


Figure 2. LM images showing the microstructures of cast irons (a) SiMo, (b) SiW and (c) SiNb.

Table 3. Image analysis results for graphite morphology as determined by DIN EN ISO 945-2 (area %).

Specimen	III  Vermicular graphite	V  Irregular spheroidal graphite	VI  Spheroidal graphite	Others
SiMo	4,7	27,8	65,3	2,2
SiW	6,0	49,6	40,7	3,7
SiNb	11,3	55,1	27,8	5,7

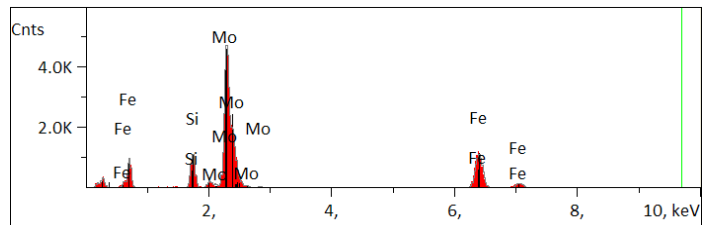
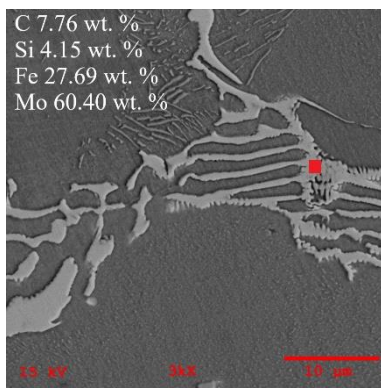


Figure 3. (a) SEM image showing the microstructure of SiMo and (b) EDS pattern taken from the carbide.

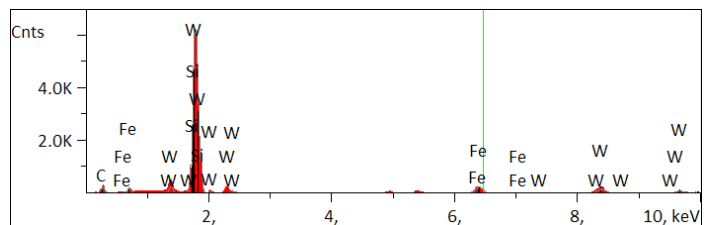
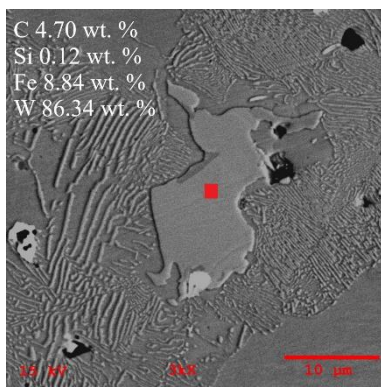


Figure 4. (a) SEM image showing the microstructure of SiW and (b) EDS pattern taken from the carbide.

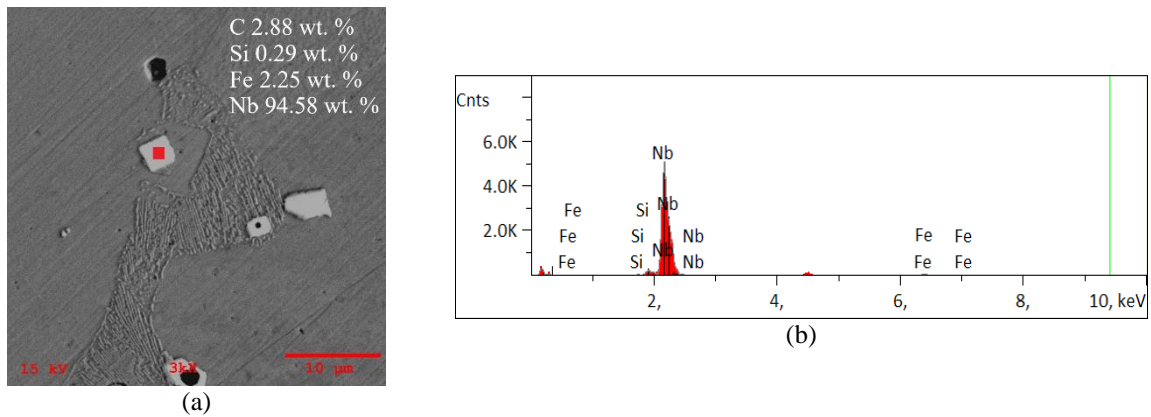


Figure 5. (a) SEM image showing the microstructure of SiNb and (b) EDS pattern taken from the carbide.

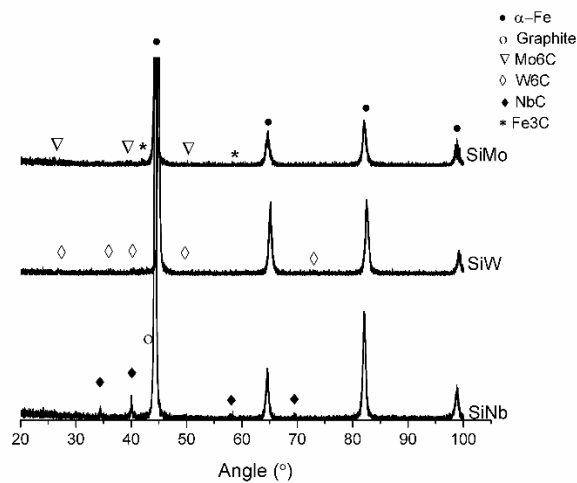


Table 4. Hardness values of specimens

Specimen	Hardness, HV1
SiMo	214,3 + 3,01
SiW	227,5 + 9,57
SiNb	216,5 + 4,15

#### 4. CONCLUSION

In this study, the ferritic ductile cast iron compositions were designed using W and Nb alloying elements to be used in place of commercial SiMo alloy at higher service temperatures. Computational alloy thermodynamics studies were carried out in order to predict the transformation temperatures and stable phases at room temperature. Alloys were cast with W and Nb additions and characterized along with commercial SiMo alloy. Experimental measurements were compared with computed results. Calculations revealed that critical transformation temperatures ( $A_1$ ) shifted to higher ones by the usage of W and Nb in place of Mo and higher Si. Calculations also indicated that expected phases at room temperature were graphite, carbide and ferrite for all compositions where the alloy carbide was  $M_6C$  for both Mo and W case, whereas it was  $MC$  type for Nb alloy. The microstructural characterizations of the cast alloys and commercial SiMo alloy showed that the predicted microstructural features i.e. ferritic matrix, graphite, carbides were present within the solidified structure and graphite morphology varied according to alloying element and Nb strongly deteriorated graphite morphology by changing it from spheroidal to irregular spheroidal and vermicular. The hardness measurements revealed that no significant difference existed between the developed alloys and commercial SiMo alloy, in that respect.

The results of this research indicated that both SiW and SiNb appear to be possible candidates to be used at higher temperature applications in place of SiMo.

### Acknowledgement

The authors, G. Aktaş Çelik, Ş. Polat and Ş. H. Atapek wish to acknowledge the financial support given by Scientific Research Projects Coordination Unit of Kocaeli University under the project no 2017/118.

### References

- [1] Y-J. Kim, H. Jang, Y-J Oh, “High-temperature low-cycle fatigue property of heat-resistant ductile-cast irons” *Metall. Mater. Trans. A*, vol. 40A, p. 2087-2097, 2009.
- [2] X Wu, G. Quan, R. Macneil, Z. Zhang, X. Liu, C. Sloss, “Thermomechanical fatigue of ductile cast iron and its life prediction”, *Metall. Mater. Trans. A*, vol. 46, no. 6, p. 2530–2543, 2015.
- [3] P. Matteis, G. Scavino, A. Castello, D. Firrao, “High-cycle fatigue resistance of Si-Mo ductile cast iron as affected by Temperature and strain rate”, *Metall and Materi Trans A*, vol.46A, p. 4086-4094, 2015.
- [4] L. M. Åberg, C. Hartung, “Solidification of SiMo nodular cast iron for high temperature applications”, *Trans Indian Inst Met* vol. 65, no.6, p.633–636, 2012.
- [5] M. Ekström, S.Jonsson,” High-temperature mechanical-and fatigue properties of cast alloys Intended for use in exhaust manifolds”, *Mater. Sci. Eng. A*, vol 616, p.78–87, 2014.
- [6] P. Matteis, G. Scavino, A. Castello, D. Firrao, High temperature fatigue properties of a Si-Mo ductile cast iron, *Procedia Mater. Sci.*, vol. 3, p. 2154-2159, 2014
- [7] D. Li, Discussion of “Microstructure and hot oxidation resistance of SiMo ductile cast irons containing Si-Mo-Al”, *Metall and Materi Trans B*, vol. 49B, p. 858-859, 2018.
- [8] M. Ekström, P. Szakalos, S. Jonsson, Influence of Cr and Ni on high-temperature corrosion behavior of ferritic ductile cast iron in air and exhaust gases, *Oxid. Met.* vol. 80, p. 455–466, 2013.
- [9] A. A. Partoaa, M. Abdolzadeh, M. Rezaeizadeh, “Effect of fin attachment on thermal stress reduction of exhaust manifold of an off road diesel engine”, *J. Cent. South Univ.* vol. 24 p. 546–559, 2017.
- [10] F. Tholence, M. Norell, High Temperature Corrosion of Cast Alloys in Exhaust Environments. II—Cast Stainless Steels, *Oxid Met*, vol. 69, p. 37–62, 2008.
- [11] J. P. Shingledecker, P. J. Maziasz, N. D. Evansa, M. J. Pollard, Creep behavior of a new cast austenitic alloy, *Int. J. Press. Vessels Pip.* vol. 84, p.21–28, 2007.
- [12] Y. Zhang, M. Li, L. A. Godlewski, J. W. Zindel, Q. Feng, Effects of W on creep behaviors of novel Nb-bearing high nitrogen austenitic heat-resistant cast steels at 1000 °C, *Mater. Charact.* vol. 139 p. 19–29, 2018.
- [13] G. E. Totten, *Steel Heat Treatment*, second ed. Portland, Longman, New York, 2006.
- [14] X. Chen, J. Xu, H. Hu, H. Mohrbacher, M. Kang, W. Zhang, A. Guo, Q. Zhai, “Effects of niobium addition on microstructure and tensile behavior of ascast ductile iron”, *Mater. Sci. Eng. A*, vol 688, p. 416-428, 2017.
- [15] A. Bedolla-Jacuinde, E. Solisand, B. Hernandez, “Effect of niobium in medium alloyed ductile cast irons”, *Int. J. Cast Met. Res.*, vol. 16, no. 5, p. 1-6, 2003.